

FFT-based 220 GHz Sparse Imaging for Target Detection

(Invited Paper)

Shaoqing Hu
 Department of Electronic and
 Electrical Engineering
 Brunel University London
 Middlesex, United Kingdom
 shaoqing.hu@brunel.ac.uk

Amir Masoud Molaei
 School of Electronics, Electrical
 Engineering and Computer Science
 Queen's University Belfast
 Belfast, United Kingdom
 A.Molaei@qub.ac.uk

Okan Yurduseven
 School of Electronics, Electrical
 Engineering and Computer Science
 Queen's University Belfast
 Belfast, United Kingdom
 okan.yurduseven@qub.ac.uk

Abstract—This paper introduces two fast imaging algorithms based on Fast Fourier Transform (FFT) for 220 GHz synthetic aperture imaging application of target detection with multi-static multiple-input and multiple-output (MIMO) array-FFT/IFFT approach and FFT matched filtering. Zero padding is proposed to improve the image quality when large sampling space is used. In addition, multi-pass synthetic aperture imaging is proposed to achieve higher image quality without increasing system cost. The 6 mm resolution at 1.4 m is achieved and reconstruction time of $200 \text{ mm} \times 200 \text{ mm}$ is as less as 0.2 s. And proposed sparse imaging with low rank matrix recovery (LRMR) technique is potential to further save system cost without comprise on high image quality.

Keywords—Fast Fourier Transform (FFT), low rank matrix recovery (LRMR), MIMO, synthetic aperture imaging, THz

I. INTRODUCTION

Millimetre wave and THz imaging is emerging for applications like personnel screening and non-destructive testing due to high resolution of short wavelength [1]–[3]. Active imaging system with multiple-input and multiple-output (MIMO) array provides a potential solution to fast imaging. However, most MIMO imaging systems use sampling spacing on the order of $\lambda/2$ meeting Nyquist sampling criterion to avoid aliasing. It incurs high cost at high operation frequency because of a large number of transceivers demanded to achieve a wide Field of view (FOV). For example, a total of 384 transmitter (Tx) antennas and 384 receiver (Rx) antennas are used in a linear personnel screening system working at 24.25-30 GHz [4]. Large element spacing between transceivers/data will help to reduce the number of transceivers and data, but it will reduce the image signal to noise ratio, decreasing its capability of detecting complex targets. To balance this conflict, multi-pass synthetic aperture imaging has been proposed based on Generalised Synthetic Aperture Focusing Technique (GSAFT) because multi-static MIMO is used, which is applicable to any MIMO topology [5]. The multi-static MIMO topology makes it impossible to directly apply Fast Fourier Transform (FFT) technique. The superposition in the GSAFT is time-consuming and this issue becomes prominent with increasing data volume.

Therefore, in this paper, two imaging algorithms based on FFT technique compatible with multi-static MIMO setup are verified in experiments for multi-pass synthetic aperture imaging at 220 GHz. The image reconstruction time reduces significantly than GSAFT-based approach so it is potential to provide real-time imaging. In addition, random sparse imaging on the basis on low rank matrix recovery (LRMR) with principal component pursuit by alternating directions method (PCPADM) has been investigated for the purpose of further reducing system cost when necessary. Different from

LRMC, LRMR also known as robust principle component analysis (RPCA) assumes a large data matrix M decomposed as a sum of low rank matrix L and sparse noise/error matrix E_δ [6]. Unlike traditional LRMR or PCA applications to recover L from measured matrix M , we proposed to make use of error matrix E_δ . This significantly improves the capability of target detection.

II. FUNDAMENTALS AND PRINCIPLES

In theory, a linear sparse periodic array (SPA) consisting of N_t Tx's and N_r Rx's is used to achieve electronic scanning in one direction. The Tx is sequentially switched on and when one is in on status, all the receivers will record/sample the echo amplitude and phase. This process is repeated when the SPA mechanically moves to next position until the planar scanning of are of interest is finished, for example, W positions are sampled as shown in Fig.1(a). N -pass datasets with a path shift d_s are phase correlated to reconstruct an improved N -pass synthetic aperture focusing image. In order to save scanning time or system cost, a sparse imaging with a random or pseudo-random samples in grey can be applied to recover the full sampling data.

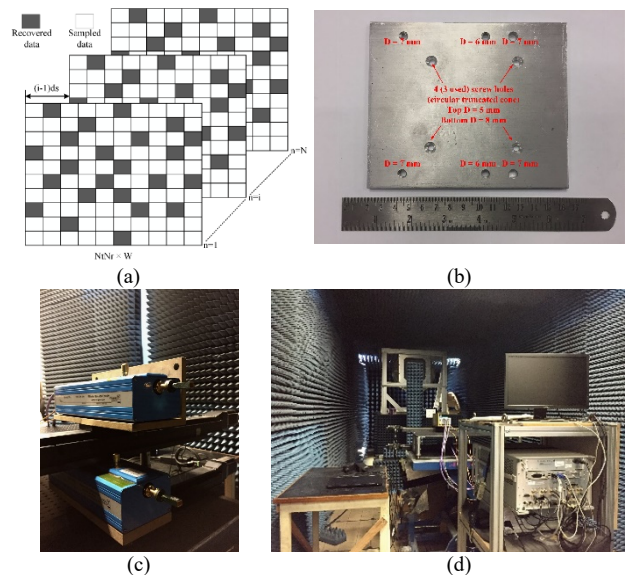


Fig.1. (a) Matrix illustration of N -pass phase correlated datasets and photos of (b) a metallic target under test (c) Tx and Rx horns on linear scanning stages (d) whole experimental imaging system

In experiment, targets such as a metallic plate in Fig.1(b) are mounted on a planar scanning system to inversely imitate the mechanical scanning of SPA. 1 Tx and 1 Rx horns on two scanning stages move to Tx and Rx positions of SPA for the purpose of achieving the horizontal electronic scanning, as shown in Fig.1(c). The peak gain of horn is about 23.81 dB at 220 GHz and the typical input power to the horn at 220 GHz

is -13 dBm (0.05 mW) [7]. The photo of whole experimental imaging system is shown in Fig.1(d).

According to robust principal component analysis theory, a low-rank matrix data L_s and error matrix data E_δ can be recovered from highly corrupted measurements/echo data $S_{obs} = P_{obs} S_{full} = P_{obs} (L_s + E_\delta)$ where P is a sparse observation matrix consisting of 1 (sampled in grey) and 0 (to be recovered in white) by solving the following problem:

$$\begin{aligned} & \text{minimise } \|L_s\|_* + \lambda_s \|E_\delta\|_1 \\ & \text{subject to } P_{obs} \cdot (L_s + E_\delta) = S_{obs} \end{aligned} \quad (1)$$

where λ_s is a scalar. $\|\cdot\|_*$ and $\|\cdot\|_1$ refer to nuclear norm and l_1 -norm, respectively. S_{full} is an approximated matrix of real samples.

After S_{full} is obtained, central interpolation is firstly applied to compensate the missing data with SPA scanning. Thereafter, multistatic-to-monostatic conversion is applied to gain a FFT compatible data so FFT-based image reconstruction approaches can be applied[3], [8]. Different from FFT/IFFT and FFT matched filtering in [3], internal zero padding, multi-pass synthetic aperture focusing, and sparse imaging are proposed and investigated in this work [7].

III. EXPERIMENTAL RESULTS

Single pass synthetic aperture imaging reconstructed by FFT/IFFT and FFT matched filtering are investigated in Fig.2. Fig.2(a) and (b) show the reconstructions without/with internal zero padding, respectively. Therefore, the sample spacing along x, y directions in Fig.2(a) are 3 mm and 4 mm, respectively while they are 0.75 mm and 1 mm in Fig.2(b). Similarly, the FFT matched filtering reconstructions without/with internal zero padding are shown in Fig.2(c) and (d). From the results, we can see the holes are clearly identified so practical 6 mm resolution is achieved. And zero padding make circular edges more smooth, real and clearer. The reconstruction time with MATLAB on a platform of Windows 10 Enterprise, Intel Core I7-10700 and random-access memory of 16 G are 0.20 s and 0.04 s with FFT/IFFT and FFT matched filtering reconstruction approach, respectively.

Besides, multi-pass synthetic aperture imaging with four-pass datasets is studied in comparison. The pass shift of SPA along electronic scanning direction is 20 mm. The reconstructed images with FFT/IFFT and FFT matched filtering approaches are compared in Fig.3. Compared to Fig.2, image quality is obviously improved so it is competent to detect more challenging targets [7]. Due to larger volume of data used, the reconstruction time increases to 0.83 s and 0.17 s with FFT/IFFT and FFT matched filtering reconstruction approach, respectively.

Finally, sparse imaging is studied by randomly turning off some elements in SPA, which provides a solution to save system cost [7]. The reconstructions with FFT/IFFT approach of 2 Tx's & 2 Rx's off and 1 Tx & 1 Rx off are shown in Fig.4(a) and (b). In comparison, the reconstructions with FFT matched filtering approach of 2 Tx's & 2 Rx's off and 1 Tx & 1 Rx off are shown in Fig.4(c) and (d). Results have demonstrated that sparse imaging is potential to provide comparable image quality with fewer data to Fig.3 reconstructed with full data. It is worth mentioning that the

initially measured full data in this experiment is already much less than the Nyquist criterion because of large sampling spacing (3 mm on electronic scanning direction and 4 mm on mechanical scanning direction) are used. Therefore, the reduction of data volume resulting from sparse imaging technique is not too high in this example.

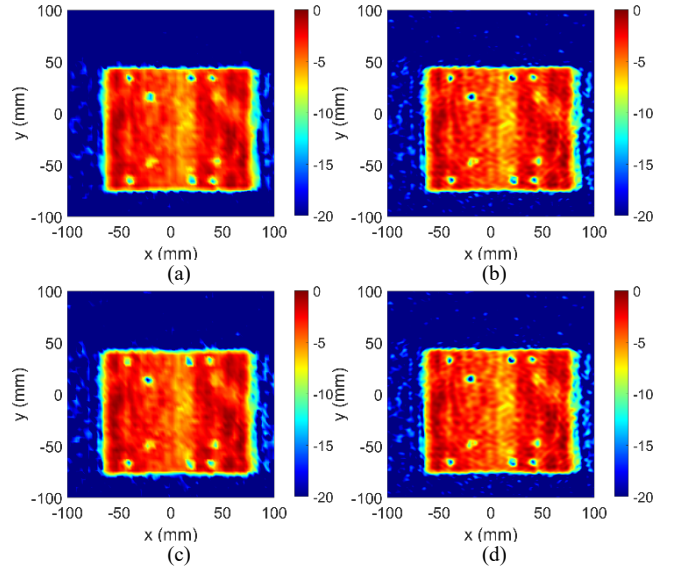


Fig.2 Single pass synthetic aperture imaging with FFT/IFFT approach (a) no internal zero padding (b) internal zero padding, and FFT matched filtering approach (c) no internal zero padding (d) internal zero padding

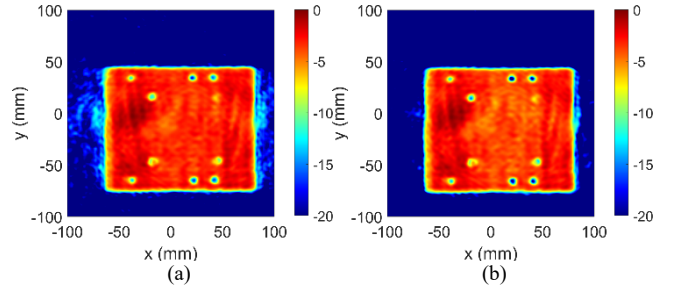


Fig.3. Four-pass synthetic aperture imaging with (a) FFT/IFFT approach and (b) FFT matched filtering approach

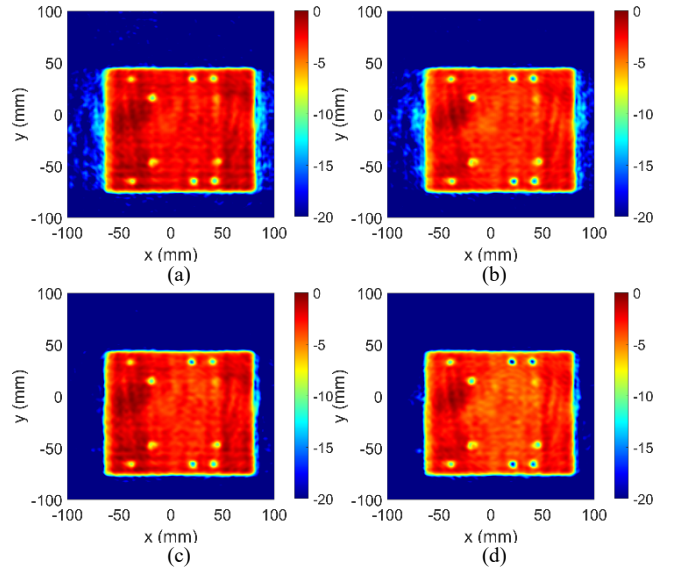


Fig.4. Four-pass synthetic aperture sparse imaging with FFT/IFFT approach of (a) 2 Tx's & 2 Rx's off (b) 1 Tx & 1 Rx off and FFT matched filtering approach of (c) 2 Tx's & 2 Rx's off (d) 1 Tx & 1 Rx off

IV. CONCLUSIONS

New FFT/IFFT and FFT matched filtering reconstruction approaches for 220GHz (THz) multi-static and multi-pass synthetic aperture imaging have been developed and experimental verified. The results show a 6 mm cross-range resolution at 1.4 m. The FFT matched filtering approach is much faster but without visible loss on image quality than FFT/IFFT approach. Besides, multi-pass synthetic aperture focusing and sparse imaging techniques are proposed to improve the imaging performance and reduce the system cost/sampling data.

REFERENCES

- [1] S. S. Ahmed, "Microwave Imaging in Security — Two Decades of Innovation," *IEEE Journal of Microwaves*, vol. 1, no. 1, pp. 191–201, 2021.
- [2] M. E. Yanik, D. Wang, and M. Torlak, "Development and Demonstration of MIMO-SAR mmWave Imaging Testbeds," *IEEE Access*, vol. 8, pp. 126019–126038, 2020.
- [3] A. M. Molaei, S. Hu, V. Skouropoliakou, V. Fusco, X. Chen, and O. Yurduseven, "Fast Processing Approach for Near-Field Terahertz Imaging with Linear Sparse Periodic Array," *IEEE Sensors Journal*, pp. 1–1, 2022.
- [4] D. Sheen, D. McMakin, and T. Hall, "Near-field three-dimensional radar imaging techniques and applications," *Applied Optics*, vol. 49, no. 19, pp. E83–E93, 2010.
- [5] S. Hu, C. Shu, Y. Alfadhil, and X. Chen, "A THz Imaging System Using Linear Sparse Periodic Array," *IEEE Sensors Journal*, vol. 20, no. 6, pp. 3285–3292, 2020.
- [6] E. J. Candès, X. Li, Y. Ma, and J. Wright, "Robust principal component analysis?," in *Journal of the ACM*, vol. 58, no. 3, pp. 11: 1–37, May 2011.
- [7] S. Hu, C. Shu, Y. Alfadhil, and X. Chen, "Advanced THz MIMO Sparse Imaging Scheme Using Multipass Synthetic Aperture Focusing and Low-Rank Matrix Completion Techniques," *IEEE Transactions on Microwave Theory and Techniques*, vol. 70, no. 1, pp. 659–669, Jan. 2022.
- [8] Z. Wang, Q. Guo, X. Tian, T. Chang, and H. L. Cui, "Near-Field 3-D Millimeter-Wave Imaging Using MIMO RMA with Range Compensation," *IEEE Transactions on Microwave Theory and Techniques*, vol. 67, no. 3, pp. 1157–1166, Mar. 2019.